Strid, Å., Nore, B. F., Nyrén, P., & Baltscheffsky, M. (1987) *Biochim. Biophys. Acta 892*, 236-244.
Strid, Å., Nyrén, P., & Baltscheffsky, M. (1988) *Eur. J. Biochem. 176*, 281-285.
Webster, G. D., Edwards, P. A., & Jackson, J. B. (1977) *FEBS Lett. 76*, 29-35.
Williams, R. J. P. (1976) *Symp. Soc. Exp. Biol. 30*, 1-17.
Williams, R. J. P. (1980) *Dev. Biochem. 14*, 3-10.

Binding of Sulfonamide and Acetamide to the Active-Site Zn^{2+} in Carbonic Anhydrase: A Theoretical Study†

Jiin-Yun Liang and William N. Lipscomb*
Gibbs Chemical Laboratories, Department of Chemistry, Harvard University, Cambridge, Massachusetts 02138
Received February 6, 1989; Revised Manuscript Received June 12, 1989

ABSTRACT: Self-consistent field molecular orbital (SCF MO) calculations at both 4-31G and STO-3G levels have been used to examine the binding conformations of sulfonamide and acetamide compounds to the active site of carbonic anhydrase. The results are as follows: (1) sulfonamide binds to the Zn^{2+} ion in its deprotonated form through the sulfonamide nitrogen to the fourth coordination site of the metal ion; (2) acetamide as neutral species binds to the basic form of the enzyme through the carbonyl oxygen to the fifth coordination site of the metal ion; and (3) the acetamidate ion binds to the acid form of the enzyme through the amide nitrogen to form a tetracoordinated metal complex with three histidine ligands. Analysis of the effects of individual active-site residues on the binding conformations of these inhibitors suggests that metal alone favors bidentate coordination of sulfonamidate and acetamidate complexes and that electron donation from three histidine ligands to the metal ion determines the formation of a tetracoordinated metal complex, which is further stabilized by the presence of Thr 199, as it receives one hydrogen bond from the sulfonamide NH^- or from the acetamide NH^- and donates a backbone NH hydrogen bond to a sulfonamide oxygen. The calculated binding conformation of sulfonamide and the hydrogen-bonding interactions between sulfonamide and the enzyme are consistent with the X-ray diffraction study of the AMSulf–HCA II complex. However, no X-ray structures are available for amide–HCA II complexes. Finally, a three-step binding mechanism is proposed to explain the experimentally observed slow association kinetics of amide compounds: (1) initial binding of an amide compound through the carbonyl oxygen to the fifth coordination site of the metal ion; (2) proton transfer from the amide nitrogen to the metal-bound OH^-; and (3) release of a metal-bound water molecule and subsequent coordination of the amidate compound through the amide nitrogen to the metal ion. The proton-transfer process of step 2 is considered to be rate limiting.

Carbonic anhydrase is a zinc metalloenzyme that catalyzes the reversible hydration of CO_2 to bicarbonate ion and a proton. In human carbonic anhydrase II (HCA II) the maximal turnover number is 10^6 s^{-1} at 25 °C. It is now widely accepted that in HCA II (Lindskog, 1983; Lindskog et al., 1984; Lipscomb, 1983; Pocker & Sarkanen, 1978; Prince, 1979; Coleman, 1980; Silverman & Lindskog, 1988) the initial nucleophilic attack occurs by a Zn^{2+}-bound hydroxide ion and that the subsequent proton transfer is catalyzed by a non-Zn^{2+}-liganded histidine or another proton-transfer group[1] (Forsman et al., 1988) and by buffer in HCA II. A plausible catalytic mechanism for the hydration of CO_2 is given in Figure 1.

It is known that tightly bound inhibitors of carbonic anhydrase are mononegative anions (e.g., halides, N_3^-, NCO^-, NCS^-, CN^-) or neutral molecules (e.g., sulfonamide) with low pK_a values that can deprotonate to form anionic species during metal binding (Pocker & Sarkanen, 1978). Other neutral inhibitors, such as alcohols, organic solvents, and amide compounds (Verpoorte et al., 1967; Pocker & Stone, 1968; Whitney et al., 1967; Whitney, 1970, 1973; Pocker & Sarkanen, 1978; Bertini & Luchinat, 1983), have high pK_a values and are in general weak inhibitors.

Sulfonamide compounds, with a pK_a of about 10 for an unbound benzenesulfonamide (Taylor & Burgen, 1971; Taylor et al., 1970, 1971; Harrington & Wilkins, 1980; King & Burgen, 1976), are known to bind specifically (K_i = 0.01–1 μM) (Kanamori & Roberts, 1983) to the zinc ion using a deprotonated form of the NH_2 group. The observed large ^{111}Cd–^{15}N spin-coupling constants between ^{15}N of sulfonamide and ^{111}Cd of ^{111}Cd-substituted HCA indicates a direct coordination of the deprotonated sulfonamidate ion through nitrogen to the Cd ion (Edelhoch et al., 1981; Blackburn et al., 1985). The early X-ray structures of acetazolamide (Diamox)–HCA I (Kannan et al., 1977; Kannan, 1979) and benzenesulfonamide–HCA I (Kannan, 1979) complexes indicated that sulfonamide binds in a bidentate conformation to the metal ion, with the sulfonamide nitrogen replacing the solvent water molecule at the fourth coordination site and one sulfonamide oxygen bound to the fifth coordination site of the metal ion. (For example, Zn–O = 2.7 Å and Zn–N = 2.8 Å in the X-ray structure of the acetazolamide–HCA I complex.) However, in the recently refined X-ray structures of the acetazolamide–HCA II complex to 3-Å resolution (Eriksson

† For support of this research we thank the National Science Foundation (CHE-85-15347, CHE-88-20590 and PCM-77-11398) and the National Institutes of Health (GM06920).

[1] Mutations of His 64 to Lys, Gln, Glu, or Ala change k_{cat} for CO_2 hydration by factors of 1.5–3.5 as compared to the value for the native enzyme at pH 8 and 25 °C.

0006-2960/89/0428-9724$01.50/0

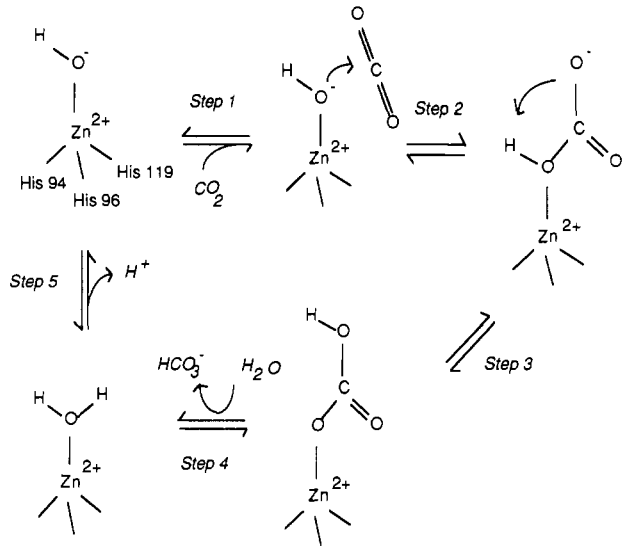

FIGURE 1: Carbonic anhydrase catalyzed CO_2 hydration consists of the following steps: (1) binding of CO_2 near Zn^{2+}; (2) conversion of CO_2 to HCO_3^- by nucleophilic attack of Zn^{2+}-bound OH^- on C of CO_2; (3) internal proton transfer of Zn^{2+}-bound HCO_3^-; (4) binding of H_2O to Zn^{2+} and ionization of this Zn^{2+}-bound H_2O (probably assisted by the negatively charged Glu 106–Thr 199 proton network) to facilitate release of HCO_3^-; and (5) coordinated transfer of H^+ from Zn^{2+}-bound H_2O to a proton-transfer group and then to buffer and then to solvent. In this mechanism, the mechanistic role of a pentacoordinated Zn^{2+} species is unclear, although such intermediates could be accommodated in several steps depicted here. In step 2, for instance, one oxygen of CO_2 could bind to Zn^{2+} at the fifth coordination site. Also, in step 4, both an OH and a terminal O of HCO_3^- could bind to Zn^{2+} before the product release.

et al., 1986, 1989), and the (acetoxymercuri)benzenesulfonamide (AMSulf)–HCA II complex to 2.0-Å resolution (Eriksson et al., 1986, 1989), a monodentate binding conformation is documented. In these more complete studies, the sulfonamide nitrogen is shown to bind to the zinc ion at Zn–N ~2.0 Å; the sulfonamide oxygen is ~3.1 Å away from the metal ion. In addition, the hydroxyl oxygen of Thr 199 receives a hydrogen bond from the NH^- group of the sulfonamidate ion, and the main-chain NH of Thr 199 is hydrogen bonded to the sulfonamide oxygen (Eriksson et al., 1989). The exact binding conformation of the sulfonamidate ion to carbonic anhydrase is perhaps most reliable in the refined AMSulf complex.

Amide compounds, with large pK_a values (approximately 14–15), have long been thought to bind to the active-site Zn^{2+} as neutral species. Spectral studies of the binding of iodoacetamide (K_i = 40 mM) and ethyl carbamate (K_i = 6.7 mM) to cobalt-substituted carbonic anhydrase have documented a direct coordination of the deprotonated amide nitrogen to the cobalt ion. This conclusion is further supported by the characteristic pH profile of the equilibrium binding constant (Rogers et al., 1987). The association rate constants of amide compounds are 1–10 M^{-1} s^{-1}, which are relatively small compared with the values of 10^6–10^9 M^{-1} s^{-1} for the sulfonamide compounds. According to Rogers et al., the slow association kinetics of amide compounds may imply an energetically unfavorable deprotonation of the amide group before final coordination to the metal ion. However, no X-ray structures are available for amide–CA complexes.

This paper applies SCF MO calculations to examine the binding conformations of sulfonamide, acetamide, and their deprotonated species to the active site of carbonic anhydrase. The effects of active-site metal ion and active-site residues, Thr 199 and His 94, 96, and 119, on the binding conformations of these inhibitors are analyzed. A three-step binding mechanism is proposed to account for the slow association kinetics of amide compounds: (1) initial binding of amide compound through the carbonyl oxygen to the fifth coordination site of the metal ion; (2) proton transfer from the amide nitrogen to the metal-bound OH^-; and (3) release of the metal-bound water molecule and subsequent coordination of the amidate compound through the amide nitrogen to the metal ion. The energy barrier of the proposed rate-limiting proton-transfer process of step 2 is estimated.

Methods

Model Compounds. To study the binding conformations of sulfonamide and amide compounds, model compounds of sulfonamide–, sulfonamidate–, acetamide–, and acetamidate–enzyme complexes, which contain various active-site components with different binding conformations, were constructed and their geometries optimized. Be^{2+} is used in the model compounds to simulate the Zn^{2+} ion. This substitution is supported by our previous studies on internal proton transfer of Zn^{2+}-bound HCO_3^- (Liang & Lipscomb, 1987), in which we found that the electrostatic interactions between the positive charges on the metal ion and those on the transferring proton are similar in both zinc-containing and beryllium-containing reactions; in addition, similar reaction paths and energy barriers[2] were obtained for the Be^{2+} and Zn^{2+} systems. The active-site residue Thr 199 is represented by CH_3OH and the backbone NH of Thr 199 by NH_3. Three NH_3 molecules are used to simulate the imidazole rings of three histidine ligands (His 94, 96, and 119). Substitution of NH_3 for imidazole is supported by the finding that NH_3 and imidazole transfer a similar amount of charge to Zn^{2+} (Pullman & Demoulin, 1979). The positions of these active-site residues were obtained from the X-ray diffraction structure of AMSulf–HCA II complex (Eriksson et al., 1989) and were fixed during geometry optimizations of the metal–inhibitor complexes.

Theoretical Methods. The SCF MO method is applied to obtain optimized molecular geometries and molecular energies of Be^{2+}–sulfonamide, Be^{2+}–sulfonamidate, Be^{2+}–acetamide, and Be^{2+}–acetamidate complexes. Complexes ⟨IA⟩, ⟨IB⟩, ⟨IC⟩, and ⟨ID⟩ and their deprotonated species (Figure 2) and complexes ⟨IIA⟩, ⟨IIB⟩, ⟨IIA$^-$⟩, ⟨IIB$^-$⟩, and ⟨IIC$^-$⟩ (Figure 3) were examined at the 4-31G level (Ditchfield et al., 1971), while complexes ⟨IF$^-$⟩, ⟨IG$^-$⟩, and ⟨IH$^-$⟩ (Figure 4) and complexes ⟨IIF⟩, ⟨IIG⟩, ⟨IIH⟩, ⟨III$^-$⟩, ⟨IIJ$^-$⟩, and ⟨IIK$^-$⟩ (Figure 5), which include active-site residues, were examined at the STO-3G level (Hehre et al., 1969). Geometry optimization of each binding conformation requires between 5 and 20 CPU h on the Cray/XMP. In this study, the models do not take into account entropy effects of the enzyme, solvent, and buffers. Thus, we regard only relative energies as significant.

Results

Binding Conformations of Sulfonamide and the Sulfonamidate Ion. Table I contains the optimized molecular geometries and molecular energies of the Be^{2+}–sulfonamide and Be^{2+}–sulfonamidate complexes (Figures 2 and 4); Table II records the corresponding Mulliken population analysis (Mulliken, 1955).

(*a*) *Effects of the Active-Site Metal Ion on the Binding Conformations.* Four stable conformers of Be^{2+}–sulfonamide complexes are obtained (Figure 2): ⟨IA⟩ with O_1 on Be^{2+};

[2] The energy barrier, as used here, is a reaction energy cost, not an activation barrier to an intermediate stage of the reaction.

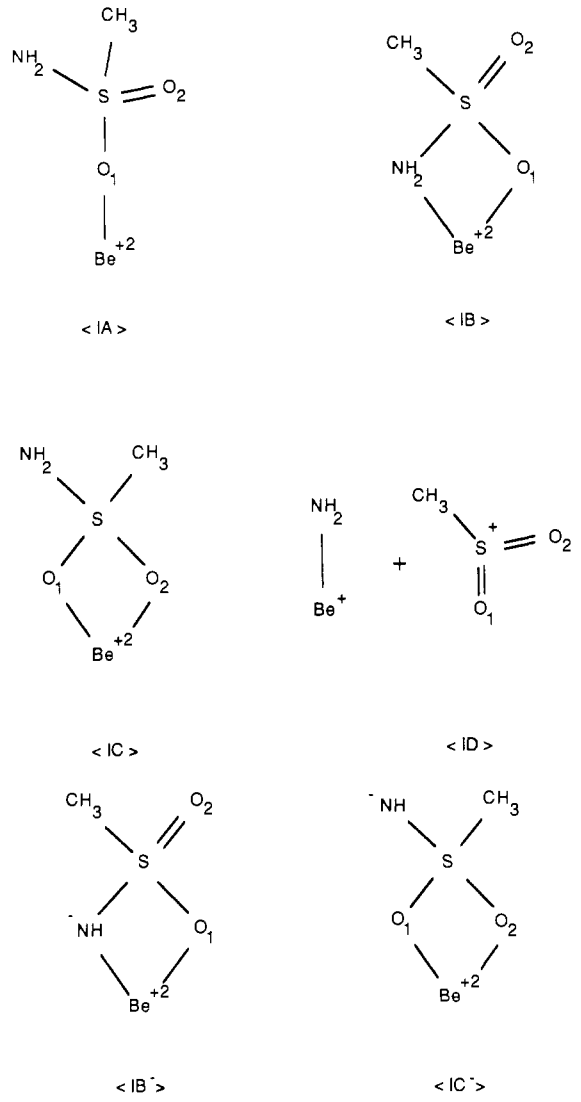

FIGURE 2: Be^{2+}–sulfonamide complexes: ⟨IA⟩ with O_1 coordinated to Be^{2+}; ⟨IB⟩ with O_1 and N coordinated to Be^{2+}; ⟨IC⟩ with O_1 and O_2 coordinated to Be^{2+}; and ⟨ID⟩ with N coordinated to Be^{2+}. In ⟨ID⟩, the C–N bond is cleaved during geometry optimization, which yields $Be(NH_2)^+$ and $CH_3SO_2^+$ segments. Be^{2+}–sulfonamidate complexes: ⟨IB⁻⟩ with O_1 and N coordinated to Be^{2+}; and ⟨IC⁻⟩ O_1 and O_2 coordinated to Be^{2+}. Be^{2+} is used in the model compounds to stimulate the active-site Zn^{2+} ion.

⟨IB⟩ with O_1 and N on Be^{2+}; ⟨IC⟩ with O_1 and O_2 on Be^{2+}; and ⟨ID⟩ with N on Be^{2+}. Among these complexes, ⟨IC⟩, with Be^{2+}–O_1 = 1.596 Å and Be^{2+}–O_2 = 1.6 Å, is most stable and is ~21 kcal/mol lower in energy than the other conformers (Table I). The S–N bond of ⟨ID⟩ is cleaved during geometry optimization, which yields $Be(NH_2)^+$ and $CH_3SO_2^+$ segments. For the Be^{2+}–sulfonamidate complex, two stable conformers, ⟨IB⁻⟩ and ⟨IC⁻⟩, are obtained (Figure 2 and Table I), of which ⟨IB⁻⟩, with Be–N = 1.758 Å and Be–O_1 = 1.523 Å, is ~23 kcal/mol lower in energy than ⟨IC⁻⟩. Structures ⟨IA⁻⟩ and ⟨ID⁻⟩ optimize directly to ⟨IC⁻⟩ and ⟨IB⁻⟩, respectively. Studies of sulfonamide ionization indicate that the deprotonation energy of 363 kcal/mol for a neutral isolated sulfonamide molecule is reduced to 103 kcal/mol when one oxygen is coordinated to the metal ion and to 79 kcal/mol when the sulfonamide nitrogen is coordinated to the metal ion.

Mulliken population analysis of the Be^{2+}–sulfonamide and Be^{2+}–sulfonamidate complexes (Table II) indicates that atoms S, Be, and H are positively charged and atoms C, O_1, O_2, and N are negatively charged. Among the negatively charged atoms, the electron population has the ordering of Q(N) (most negative) > $Q(O_1) \sim Q(O_2) > Q$(C) (most positive). Coordination of O and/or N to Be^{2+} is shown to lengthen the bond lengths between sulfur and metal-coordinated heavy atoms and to shorten those between sulfur and non-metal-coordinated heavy atoms (Table I). This change in geometry is accompanied by transfer of a total of 0.5–0.75 electrons from non-metal-coordinated heavy atoms through sulfur to metal-coordinated heavy atoms and then to the metal ion (Table II). During this electron redistribution, charge variations on the sulfonamide nitrogen and methyl carbon are relatively small compared to those on the other heavy atoms. This feature may reflect the flexible electron transfer from amide hydrogens and methyl hydrogens to the amide nitrogen and methyl carbon, respectively. This transfer stabilizes the electron populations of N and C in sulfonamide.

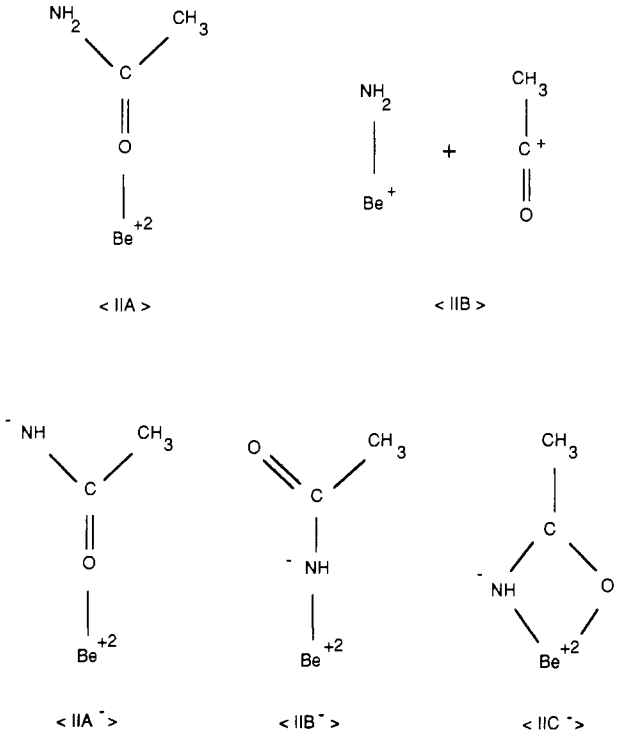

FIGURE 3: Be^{2+}–acetamide and Be^{2+}–acetamidate complexes: ⟨IIA⟩ and ⟨IIA⁻⟩, with the carbonyl oxygen coordinated to Be^{2+}; ⟨IIB⟩ and ⟨IIB⁻⟩, with the amide nitrogen coordinated to Be^{2+}; and ⟨IIC⁻⟩, with both carbonyl oxygen and the amide nitrogen coordinated to Be^{2+}. In ⟨IIB⟩, the N–C bond is cleaved during geometry optimization, which yields $Be(NH_2)^+$ and CH_3CO^+ segments. See legend of Figure 4.

(*b*) *Effects of the Active-Site Residues on the Binding Conformations.* In complex ⟨IF⁻⟩, three histidine ligands are included in the study of binding conformation of the sulfonamidate ion (Figure 4). Electron transfer of ~0.8 electrons from three histidine ligands to the metal ion is shown to weaken the Be^{2+}–O_1 interaction observed in complex ⟨IC⁻⟩; as a result, only the sulfonamide nitrogen is coordinated to the metal ion (Be^{2+}–O_1 = 2.56 Å and Be^{2+}–N = 1.64 Å, Table I) to form a tetracoordinated metal complex. In complex ⟨IG⁻⟩ in the presence of Thr 199 (Figure 4), a bidendate binding conformation with Be^{2+}–O_1 = 1.54 Å and Be^{2+}–N = 1.51 Å (Table I) is obtained. In this conformation the OH group of Thr 199 receives a hydrogen bond from the NH group of the sulfonamidate ion. In complex ⟨H⁻⟩ (Figure 4), both Thr 199 and three histidine ligands are present, and the sulfonamidate ion binds to the fourth coordination site of the metal ion with Be^{2+}–O_1 = 2.1 Å and Be^{2+}–N = 1.65 Å (Tables I and III). In addition, the hydroxyl oxygen of Thr 199 receives a hydrogen bond from the NH group of the sulfonamidate ion

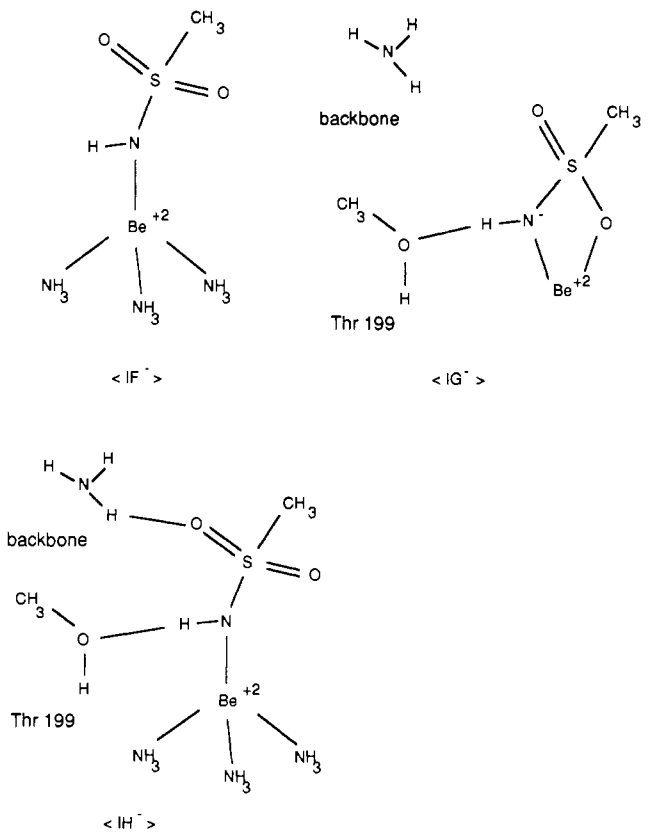

FIGURE 4: Be^{2+}–sulfonamidate complexes in the presence of various active-site residues: ⟨IF⁻⟩ contains His 94, 96, and 119; ⟨IG⁻⟩ contains Thr 199; and ⟨IH⁻⟩ contains both Thr 199 and three histidine ligands. The active-site residue Thr 199 is represented by CH_3OH and the backbone NH of Thr 199 by NH_3; the imidazole rings of three histidine ligands are represented by three NH_3 molecules. The positions of these active-site residues are obtained from the X-ray structures of the AMSulf–HCA II complex (Eriksson, 1988; Eriksson et al., 1989).

(NH···O = 2.7 Å and N–H–O = 159°), and the main-chain NH of Thr 199 is hydrogen bonded to the non-metal-liganded sulfonamide oxygen (O···NH = 2.8 Å and O–H–N = 165.0°). These hydrogen bonds in complex ⟨H⁻⟩ are consistent with those observed in the X-ray structure of AMSulf–HCA II (Eriksson, 1988).

Binding Conformations of Acetamide and the Acetamidate Ion to Carbonic Anhydrase. (a) Effects of the Active-Site Metal Ion on the Binding Conformations. Three binding conformations of Be^{2+}–acetamide and Be^{2+}–acetamidate complexes were examined (Figure 3 and Table IV): ⟨IIA⟩ and ⟨IIA⁻⟩ with the carbonyl oxygen on Be^{2+}; ⟨IIB⟩ and ⟨IIB⁻⟩ with the amide nitrogen on Be^{2+}; and ⟨IIC⟩ and ⟨IIC⁻⟩ with both the carbonyl oxygen and amide nitrogen on Be^{2+}. The most stable Be^{2+}–acetamide complex is ⟨IIA⟩ with Be–O = 1.392 Å (⟨IIA⟩, Figure 3). The C–N bond of ⟨IIB⟩ is cleaved during geometry optimization, yielding $Be(NH_2)^+$ and CH_3CO^+ segments; ⟨IIC⟩ optimizes directly to ⟨IIA⟩. The most stable Be^{2+}–acetamidate complex is ⟨IIC⁻⟩, with Be–O = 1.557 Å and Be–N = 1.610 Å (⟨IIC⁻⟩, Figure 3). The complex ⟨IIC⁻⟩ is ~50 kcal/mol more stable than ⟨IIA⁻⟩ and ⟨IIB⁻⟩ (Table IV). Studies of acetamide ionization indicate that the deprotonation energy of 392 kcal/mol for an isolated neutral acetamide molecule is reduced to 151 kcal/mol when the carbonyl oxygen is coordinated to the Be^{2+} ion.

(b) Effects of the Active-Site Residues on the Binding Conformations. When active-site residues are included in complexes ⟨IIE⟩, ⟨IIF⟩, ⟨IIG⟩, and ⟨IIH⟩ (Figure 5), a consistent binding conformation of the acetamide molecule with the carbonyl oxygen coordinated to the fifth coordination

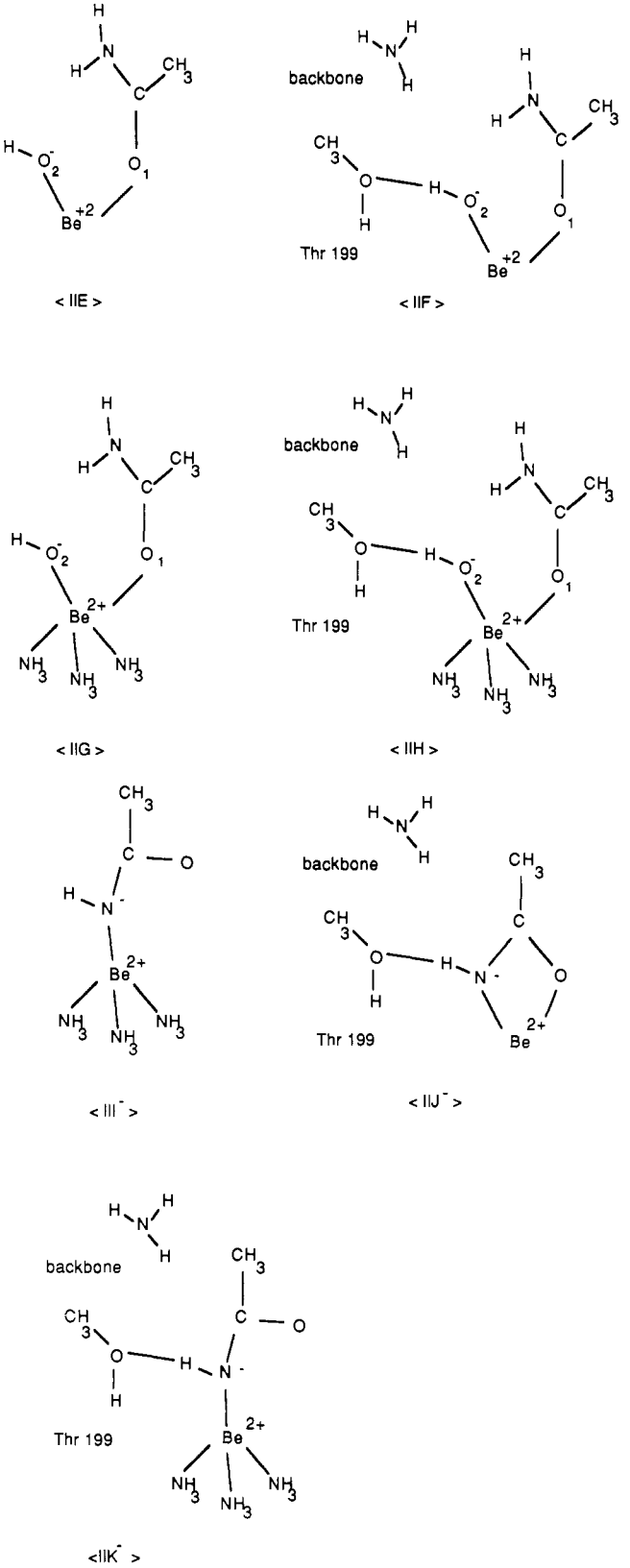

FIGURE 5: Be^{2+}–acetamide and Be^{2+}–acetamidate complexes in the presence of various active-site components: ⟨IIE⟩ contains the OH^- ligand; ⟨IIF⟩, the OH^- ligand and Thr 199; ⟨IIG⟩, the OH^- ligand, His 94, 96, and 119; ⟨IIH⟩, the OH^- ligand, Thr 199, His 94, 96, and 119; ⟨III⁻⟩, Thr 199; ⟨IIJ⁻⟩, His 94, 96, and 119; and ⟨IIK⁻⟩, Thr 199, His 94, 96, and 119 See legend of Figure 4.

site of the metal ion is observed. Electron transfer from metal ligands to the metal ion is shown to reduce the interactions between the acetamide molecule and the metal ion. These changes lead to increase of the Be^{2+}–O distance from 1.392

Table I: Molecular Geometries and Energies of the Be^{2+}–Sulfonamide and Be^{2+}–Sulfonamidate Complexes[a]

	⟨IA⟩	⟨IB⟩	⟨IC⟩	⟨ID⟩	⟨IE⟩
S–C	1.865	1.910	1.916	1.901	1.815
S–O_1	1.673	1.678	1.714	1.523	1.614
S–O_2	1.623	1.586	1.715	1.523	1.614
S–N	1.634	1.898	1.627		1.713
BE–O_1	1.399	1.523	1.596		
BE–O_2	3.662	3.495	1.600		
BE–N	3.875	1.758	3.518	1.450	
O_1–S–C	101.6	109.1	114.2	117.6	107.9
O_2–S–C	118.2	119.5	114.9	117.6	107.9
N–S–C	109.1	113.0	111.8		103.2
H_1–N–S	122.0	115.7	120.1		113.8
H_2–N–S	117.7	109.0	120.6		113.9
H_1–N–S–H_2	183.2	238.4	178.9		139.1
energy	20.7	21.6	0.0	14.8	

	⟨IB^-⟩	⟨IC^-⟩	⟨IE^-⟩	⟨IF^-⟩	⟨IG^-⟩	⟨IH^-⟩
S–C	1.839	1.853	1.809	1.813	1.820	1.817 (1.88)
S–O_1	1.709	1.714	1.628	1.764	1.740	1.822 (1.45)
S–O_2	1.600	1.747	1.628	1.776	2.048	1.725 (1.45)
S–N	1.749	1.639	1.719	1.762	1.723	1.732 (1.59)
BE–O_1	1.550	1.554		2.560	1.543	2.081 (3.14)
BE–O_2	3.524	1.528		3.312	3.912	4.102 (4.17)
BE–N	1.569	3.394		1.642	1.510	1.650 (2.01)
O_1–S–C	105.5	107.0	104.2	119.5	103.0	109.5 (118.3)
O_2–S–C	114.2	104.2	104.2	112.1	117.0	109.3 (117.9)
N–S–C	112.0	125.5	98.9	107.2	105.1	105.0 (121.4)
H_1–N–S	120.7	111.8	105.7	104.9	115.2	107.3
H_1–N–S–Be	−168.4					
N199–O_2					3.478	2.8 (3.12)
O199–N					2.655	2.7 (2.76)
energy	0.0	23.2				

[a] The bond lengths are in angstroms, bond angles in degrees, and energies in kcal/mol. The binding conformations of the Be^{2+}–sulfonamide complexes ⟨IA⟩, ⟨IB⟩, ⟨IC⟩, and ⟨ID⟩ and of the Be^{2+}–sulfonamidate complexes ⟨IB^-⟩ and ⟨IC^-⟩ are shown in Figure 2. ⟨IE⟩ is the neutral sulfonamide molecule and ⟨IE^-⟩ the sulfonamidate ion. ⟨IF^-⟩ has, in addition to the Be^{2+}–sulfonamidate complex, three histidine ligands; ⟨IG^-⟩ has Thr 199; and ⟨IH^-⟩ has both three histidine ligands and Thr 199 (Figure 4). Except ⟨IF^-⟩, ⟨IG^-⟩, and ⟨IH^-⟩ that are examined at the STO-3G level, other complexes are analyzed at the 4-31G level. O199–N is the distance between the hydroxyl oxygen of Thr 199 and the sulfonamide nitrogen of the sulfonamidate ion, and N199–O is the distance between the backbone NH of Thr 199 and the sulfonamide oxygen. We assume here N–H = 1.0 Å, C–H = 1.0 Å, and CH_3 has C_3 symmetry. The values included in the parentheses under column ⟨IH^-⟩ are the geometries obtained from the X-ray structure of the AMSulf–HCA II complex (Eriksson, 1988; Eriksson et al., 1989). The listed molecular energies are relative to that of the most stable conformer among the related complexes.

Å in ⟨IIA⟩ to 1.513 Å in ⟨IIE⟩, 1.517 Å in ⟨IIF⟩, 1.785 Å in ⟨IIG⟩, and 2.993 Å in ⟨IIH⟩ (Figure 5 and Table IV). In the binding of the acetamidate ion, on the other hand, inclusion of Thr 199 in ⟨III^-⟩ yields a bidentate binding conformation (Figure 5), while inclusion of three histidine ligands in ⟨IIJ^-⟩ and ⟨IIK^-⟩ favors the monodentate binding conformation in a tetracoordinated metal complex. The amide group of the acetamide ion donates a hydrogen bond to the OH group of Thr 199 (Figure 5).

Mulliken population analysis (Mulliken, 1955) of Be^{2+}–acetamide and Be^{2+}–acetamidate complexes indicates that the amide nitrogen when coordinated to the metal ion is the most negatively charged atom of the acetamide ligand (Table V).

Proton Transfer from the Acetamide Nitrogen to the Be^{2+}-Bound OH^-. In the proposed three-step binding mechanism of amide compounds (see the introduction and Figure 6), the proton-transfer process of step 2 is considered to be the rate-limiting step. The reaction energy profiles of this proton-transfer process have been traced at the 4-31G SCF MO level. The energy barrier is 29.1 kcal/mol (Table VI) for proton transfer from the acetamide nitrogen to the metal-bound OH^- in the $Be^{2+}(OH^-)CH_3CONH_2$ complex, with the reactant, $Be^{2+}(OH^-)(CH_3CONH_2)$, being the lowest energy state, and the product, $Be^{2+}(H_2O)(CH_3CONH^-)$, the highest energy state. Inclusion of Thr 199 is shown to raise the energy barrier slightly to 31.7 kcal/mol, while inclusion of three histidine ligands reduces the energy barrier to 5.9 kcal/mol. Qualitatively similar results are obtained in the STO-3G calculations. The barriers are 16.5 kcal/mol in the presence of the metal ion, 17.4 kcal/mol in the presence of Thr 199, −8.9 kcal/mol in the presence of three histidine ligands, and 18.9 kcal/mol in the presence of both Thr 199 and three histidine ligands. The STO-3G barriers are systematically lower than the corresponding 4-31G barriers by ~13 kcal/mol (Table VI). These results suggest that although STO-3G calculations are unable to estimate the absolute energy barriers for the proton-transfer processes, the relative energy differences obtained at the STO-3G level among different reaction systems are consistent with those obtained with the 4-31G basis set. Thus, STO-3G calculations may be useful in understanding the catalytic effects of active-site residues in large enzyme systems.

Discussion

Mulliken population analysis of Be^{2+}–sulfonamide and Be^{2+}–sulfonamidate complexes (Table II) indicated that the sulfonamide nitrogen has more negative charge than the sulfonamide oxygen.[3] This result, although contradictory to

[3] The only exception is conformer ⟨IC^-⟩, in which the two metal-coordinated oxygen atoms have more electrons than the nitrogen atom. The presence of a large electron population on the oxygen atoms is probably due to participation of two lone pairs of the deprotonated nitrogen to form π-bonds with d orbitals of sulfur. This participation leaves fewer electrons on the nitrogen atom. Also, electron withdrawal from the rest of the molecule through two metal-coordinated oxygens to the metal ion leads to electron accumulation on metal-coordinated oxygen atoms.

Table II: Mulliken Population Analysis of Be^{2+}–Sulfonamide and Be^{2+}–Sulfonamidate Complexes[a]

	⟨IA⟩	⟨IB⟩	⟨IC⟩	⟨ID⟩	⟨IE⟩
atomic charge					
S	1.657	1.482	1.454	1.626	1.579
C	−0.593	−0.579	−0.558	−0.624	−0.624
H	0.304	0.312	0.350	0.339	0.244
H	0.342	0.347	0.350	0.337	0.244
H	0.329	0.373	0.343	0.345	0.256
O_1	−1.013	−0.776	−0.692	−0.512	−0.758
O_2	−0.532	−0.493	−0.687	−0.511	−0.758
N	−1.005	−1.098	−0.977	−1.03	−1.004
H	0.489	0.493	0.514	0.41	0.410
H	0.509	0.509	0.516	0.41	0.410
BE	1.516	1.429	1.388	1.20	
bond order					
S–C	0.215	0.164	0.185	0.178	0.179
S–O_1	−0.147	0.037	0.110	0.122	0.134
S–O_2	0.161	0.128	0.116	0.123	0.134
S–N	0.077	0.048	0.097		0.015
BE–O_1	0.315	0.237	0.211		
BE–O_2	0.002	0.003	0.208		
BE–N	0.000	0.132	0.001	0.462	

	⟨IB⁻⟩	⟨IC⁻⟩	⟨IE⁻⟩	⟨IF⁻⟩	⟨IG⁻⟩	⟨IH⁻⟩
atomic charge						
S	1.472	1.318	1.488	0.680	0.744	0.690
C	−0.622	−0.612	−0.615	−0.338	−0.329	−0.342
H	0.299	0.300	0.199	0.142	0.160	0.133
H	0.278	0.305	0.199	0.128	0.163	0.132
H	0.315	0.288	0.192	0.144	0.155	0.114
O_1	−0.795	−0.750	−0.882	−0.360	−0.252	−0.374
O_2	−0.605	−0.782	−0.882	−0.322	−0.117	−0.291
N	−1.080	−0.712	−0.959	−0.479	−0.505	−0.528
H	0.444	0.383	0.261	0.151	0.284	0.202
H						
BE	1.295	1.264		0.448	0.643	0.443
bond order						
S–C	0.183	0.144	0.163	0.246	0.252	0.242
S–O_1	0.146	0.027	0.109	0.081	0.154	0.063
S–O_2	0.064	0.089	0.109	0.090	0.023	0.114
S–N	0.098	0.156	0.162	0.200	0.212	0.210
BE–O_1	0.228	0.230		0.033	0.259	0.109
BE–O_2	0.002	0.247		0.000	0.000	0.000
BE–N	0.233	0.003		0.306	0.371	0.307

[a] The atomic charges are in electrons. The bond orders are in numbers of electrons, and negative bond orders indicate antibonding interactions. See Figures 2–4 and footnotes of Table I.

Table III: Comparison of the Binding Angles in the Tetracoordinated Metal Complex ⟨IH⁻⟩ and in the X-ray Structure of the AMSulf–HCA II Complex[a]

angles	θ_1	θ_2
N–Be–His 94	101.1	110.2
N–Be–His 96	96.0	119.8
N–Be–His 119	126.1	104.3
His 94–Be–His 96	106.8	106.8
His 94–Be–His 119	114.0	114.0
O–Be–His 94	77.5	85.7
O–Be–His 96	175.3	164.6
O–Be–His 119	78.2	79.6

[a] N represents the sulfonamide nitrogen and O the sulfonamide oxygen. θ_1 is the angle in the metal complex ⟨IH⁻⟩ and θ_2 the angle in the X-ray structure of the AMSulf–HCA II complex (Eriksson, 1988; Eriksson et al., 1989). See complex ⟨IH⁻⟩ in Figure 4.

the knowledge that oxygen is more electronegative than nitrogen, can be explained by the following considerations. (1) Transfer of a total of 0.5–1.0 electron (Table II) from amide hydrogens to amide nitrogen renders the nitrogen atom electron rich. (2) Two lone pairs on oxygen, while only one lone pair on nitrogen, are involved in π-bonding with d orbitals on sulfur; as a result, fewer electrons remain on oxygen than on nitrogen (Cruickshank, 1961). In the sulfonamide molecule (⟨IE⟩,

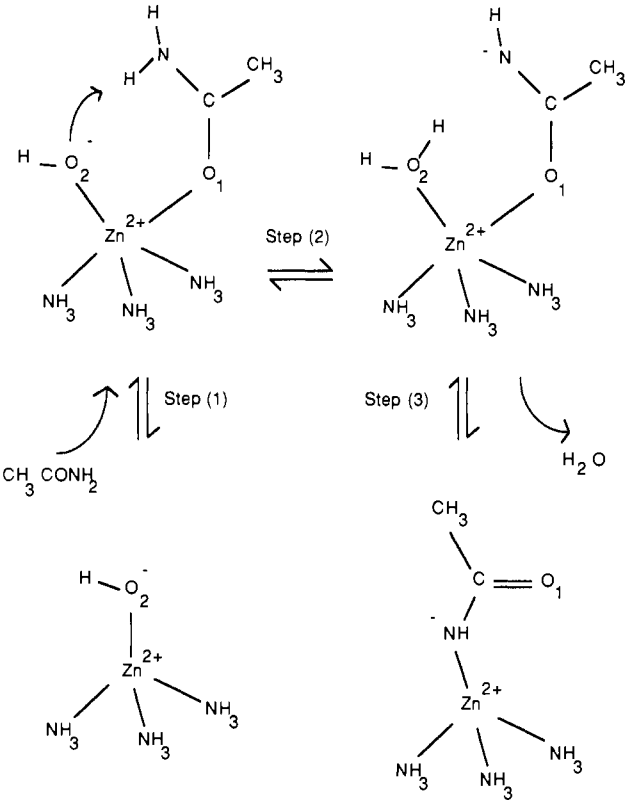

FIGURE 6: Three-step binding mechanism of amide compounds, which involves (1) initial binding of the amide compound through the carbonyl oxygen to the fifth coordination site of the metal ion, (2) proton transfer from the amide nitrogen to the metal-bound OH^- to form metal-bound H_2O and metal-bound amidate compound, and (3) release of the metal-bound water molecule and subsequent coordination of the deprotonated amidate compound through the amide nitrogen to the metal ion.

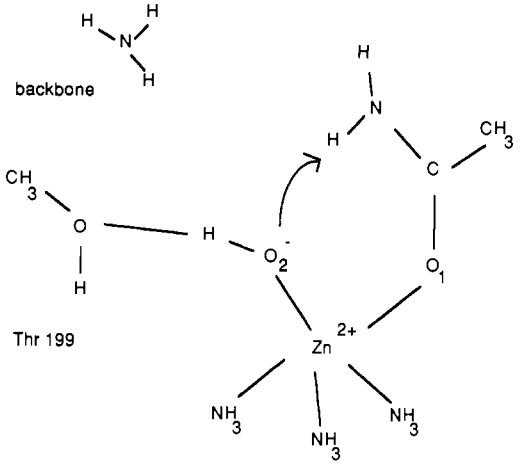

FIGURE 7: Active-site configuration in the studies of proton transfer from the amide nitrogen to the metal-bound OH^- in step 2 of Figure 6. See legend of Figure 4.

Table II), the larger bond order of 1.2 for S–O compared to 0.8 for S–N reflects the stronger π-bonding between O and S than between N and S. (3) Coordination of metal ion to the sulfonamide nitrogen withdraws electrons (0.7 electron in conformer ⟨IB⁻⟩, Table II) from the rest of the molecule through metal-coordinated nitrogen to the metal ion; thus, there is electron accumulation on the nitrogen atom. The finding that the nitrogen atom is more negatively charged than the oxygen atom in the isolated sulfonamidate ion (⟨IE⁻⟩, Table II) may account for the coordination of the sulfonamide nitrogen, rather than the sulfonamide oxygen, to the metal ion.

Table IV: Molecular Geometries and Energies of the Be^{2+}–Acetamide and Be^{2+}–Acetamidate Complexes[a]

	⟨IIA⟩	⟨IIB⟩	⟨IID⟩	⟨IIA⁻⟩	⟨IIB⁻⟩	⟨IIC⁻⟩	⟨IID⁻⟩
C–C	1.496	1.454	1.507	1.497	1.500	1.476	1.533
C–O_1	1.329	1.106	1.221	1.427	1.199	1.340	1.273
C–N	1.277		1.354	1.233	1.433	1.318	1.305
BE–O_1	1.392			1.346	3.674	1.557	
BE–N	3.542	1.450		3.576	1.464	1.610	
O_1–C–C	119.1	179.9	122.7	113.1	125.3	122.7	116.8
N–C–C	123.4		115.4	126.0	115.9	130.6	114.2
H_1–N–C	123.3		118.8	121.5	109.0		110.1
H_2–N–C	121.2		122.8			126.4	
H_2–N–C–H_1	180.1	180.0	179.9				
energy	52.9	0.0		51.4	55.8	0.0	

	⟨IIE⟩	⟨IIF⟩	⟨IIG⟩	⟨IIH⟩	⟨III⁻⟩	⟨IIJ⁻⟩	⟨IIK⁻⟩
C–C	1.534	1.535	1.540	1.543	1.513	1.546	1.538
C–O_1	1.280	1.273	1.270	1.220	1.307	1.227	1.221
C–N	1.335	1.333	1.342	1.446	1.363	1.410	1.413
BE–O_1	1.513	1.517	1.785	2.993	1.557	3.008	2.265
BE–N	3.051	3.091	2.991	4.432	1.587	1.563	1.575
O_1–C–C	119.5	119.3	119.7	123.5	117.6	122.2	118.9
N–C–C	120.1	119.1	119.4	115.5	137.3	115.3	118.1
H_1–N–C	114.3	117.9	111.7	111.2			
H_2–N–C	122.2	119.2	119.5	110.7	124.1	110.6	110.5
O199–N					2.735		2.957
O199–O_2		2.543		2.366			

[a] Figure 3 contains molecular geometries of complexes ⟨IIA⟩, ⟨IIB⟩, ⟨IIA⁻⟩, ⟨B⁻⟩, and ⟨IIC⁻⟩ and Figure 5 complexes ⟨IIE⟩, ⟨IIF⟩, ⟨IIG⟩, ⟨IIH⟩, ⟨III⁻⟩, ⟨IIJ⁻⟩, and ⟨IIK⁻⟩. In ⟨IIA⟩ and ⟨IIA⁻⟩, acetamide is coordinated to Be^{2+} at the carbonyl oxygen; in ⟨IIB⟩ and ⟨IIB⁻⟩, at the amide nitrogen; and in ⟨IIC⁻⟩, at both the carbonyl oxygen and the amide nitrogen. ⟨IID⟩ and ⟨IID⁻⟩ are the acetamide molecule and the acetamidate ion, respectively. ⟨IIE⟩, ⟨IIF⟩, ⟨IIG⟩, and ⟨IIH⟩ are the binding complexes of acetamide in the presence of various active-site components, and ⟨III⁻⟩, ⟨IIJ⁻⟩ and ⟨IK⁻⟩ are the corresponding binding complexes of the acetamidate ion. See Figures 4 and 5 and footnotes of Table I.

Table V: Mulliken Population Analysis of the Be^{2+}–Acetamide and Be^{2+}–Acetamidate Complexes[a]

	⟨IIA⟩	⟨IIB⟩	⟨IID⟩	⟨IIA⁻⟩	⟨IIB⁻⟩	⟨IIC⁻⟩	⟨IID⁻⟩	⟨IIE⟩	⟨IIF⁻⟩
atomic charge									
C	0.916	0.730	0.730	0.626	0.716	0.728	0.573	0.282	0.323
C	−0.474	−0.493	−0.504	−0.446	−0.521	−0.486	−0.467	−0.292	−0.293
H	0.246	0.331	0.211	0.171	0.268	0.265	0.877	0.097	0.113
H	0.293	0.331	0.185	0.238	0.196	0.253	0.874	0.110	0.094
H	0.293	0.331	0.185	0.238	0.196	0.253	0.874	0.099	0.097
O_1	−0.949	−0.231	−0.639	−0.901	−0.499	−0.733	−0.844	−0.390	−0.324
N	−0.793	−1.026	−0.921	−0.563	−1.017	−0.941	−0.841	−0.486	−0.488
H	0.471	0.413	0.385	0.340	0.429	0.425	0.796	0.143	0.167
H	0.486	0.413	0.370						
BE	1.513	1.200		1.297	1.233	1.236		0.526	0.456
bond order									
C–C	0.279	0.166	0.303	0.292	0.288	0.264	0.276	0.351	0.351
C–O_1	0.175	0.599	0.556	−0.006	0.562	0.248	0.439	0.350	0.433
C–N	0.364		0.100	0.605	0.042	0.212	0.396	0.463	0.373
BE–O_1	0.319			0.414	0.000	0.257		0.219	0.000
BE–N	−0.001	0.462		−0.000	0.431	0.256		−0.003	0.371

	⟨IIE⟩	⟨IIF⟩	⟨IIG⟩	⟨IIH⟩	⟨III⁻⟩	⟨IIJ⁻⟩	⟨IIK⁻⟩
atomic charge							
C	0.454	0.456	0.357	0.327	0.422	0.315	0.323
C	−0.280	−0.281	−0.288	−0.292	−0.282	−0.291	−0.293
H	0.143	0.142	0.112	0.109	0.160	0.112	0.113
H	0.141	0.141	0.116	0.114	0.151	0.098	0.094
H	0.141	0.140	0.116	0.108	0.156	0.100	0.097
O_1	−0.310	−0.309	−0.335	−0.288	−0.268	−0.322	−0.324
N	−0.406	−0.408	−0.476	−0.426	−0.418	−0.484	−0.488
H	0.302	0.308	0.305	0.193			
H	0.274	0.264	0.206	0.191	0.261	0.153	0.167
BE	0.678	0.659	0.507	0.449	0.810	0.461	0.456
bond order							
C–C	0.360	0.361	0.355	0.352	0.351	0.350	0.351
C–O_1	0.409	0.414	0.393	0.443	0.352	0.431	0.433
C–N	0.449	0.446	0.432	0.338	0.425	0.372	0.373
BE–O_1	0.288	0.283	0.176	0.007	0.237	−0.000	0.000
BE–N	−0.008	−0.007	−0.006	−0.000	0.300	0.371	0.371
BE–O_2	0.352	0.367	0.264	0.342			

[a] See footnotes of Tables II and IV.

According to the 2 Å resolution X-ray structure of the AMSulf–HCA II complex (Eriksson, 1988; Eriksson et al., 1989), the sulfonamidate ion binds to the fourth coordination site of the metal ion through the sulfonamide nitrogen, which donates a hydrogen bond to the OH group of Thr 199 (⟨IH⁻⟩, Figure 4). One sulfonamide oxygen is ~3.1 Å away from

Table VI: Energy Barriers of Proton Transfer from the Acetamide Nitrogen to the Metal-Bound OH^- (Step 2 of Figure 6)

basis	active-site configuration	energy (kcal/mol)
4-31G	Be^{2+}	29.1
	Be^{2+}-Thr 199	31.7
	$Be^{2+}(NH_3)_3$	5.9
STO-3G	Be^{2+}	16.5
	Be^{2+}-Thr 199	17.4
	$Be^{2+}(NH_3)_3$	−8.9
	$Be^{2+}(NH_3)_3$-Thr 199	18.9

Zn^{2+}; this oxygen makes van der Waals contact with Val 121 and 143. A second sulfonamide oxygen is hydrogen bonded to the backbone NH of Thr 199, and the hydrophobic group of AMSulf is in van der Waals contact with Val 121, Val 143, Leu 198, and Gln 92. In Table III and in the last two columns of Table I, we compare the calculated geometries of complex ⟨IH⁻⟩ with the X-ray structure of the AMSulf–HCA II complex. The results indicate that despite differences in bond lengths and bond angles between the Be^{2+}-containing complex ⟨IH⁻⟩ and the Zn^{2+}-containing AMSulf–HCA II complex, the overall binding conformations of the sulfonamidate ion are similar in these two complexes. Analogous binding conformations were also observed in Vedani and Dunitz's (1985) molecular mechanics simulations of sulfonamide bindings to HCA II.

In the X-ray structures of AMSulf–HCA II and Diamox–HCA II complexes, the inhibitors AMSulf and Diamox, although possessing different hydrophobic groups, are shown to share a similar binding conformation of the sulfonamidate group (Eriksson, 1988; Eriksson et al., 1989). This result suggests that the hydrophobic interaction between the hydrophobic group of sulfonamide and the enzyme has little effect on the binding conformation of the sulfonamidate group to the metal ion. Extreme cases, in which binding of the hydrophobic group alters the binding conformation of the sulfonamidate group, are, however, to be expected. In the 2.0 Å resolution X-ray structure of bovine carbonic anhydrase III (BCA III), the presence of a phenylalanine in BCA III instead of a leucine in HCA II at position 198 and the presence of an arginine instead of an histidine at position 67 are shown to significantly reduce the volume of the active-site cavity of BCA III (Eriksson, 1988). These substitutions also affect the space available in the hydrophobic pocket for sulfonamidate binding; as a result, aromatic sulfonamides (e.g., chlorzolamide) bind weakly to BCA III (Sanyal et al., 1982).

From our studies of the effects of active-site residues on the binding conformation of the sulfonamide ion, we find that (1) the metal ion alone favors the bidentate binding conformation with both N and O on the metal ion (⟨IB⁻⟩, Figure 2), (2) the presence of three histidine ligands, which donate electrons to the metal ion, leads to the formation of a tetracoordinated metal complex (⟨IF⁻⟩, Figure 4), and (3) the presence of Thr 199, which receives a hydrogen bond from the NH group of the sulfonamide ion, favors the bidentate binding conformation of the sulfonamidate ion in the absence of three histidine ligands (⟨IG⁻⟩, Figure 4). In the presence of three histidine ligands, however, the backbone NH of Thr 199 forms an additional hydrogen bond to one sulfonamide oxygen, which stabilizes the tetracoordinated metal complex (⟨IH⁻⟩, Figure 4). Thus, in the presence of Thr 199, inclusion of three histidine ligands shifts the preference of the sulfonamidate ion from forming a metal–oxygen bond in complex ⟨IG⁻⟩ to forming a hydrogen bond between the sulfonamide oxygen and the backbone NH of Thr 199 in complex ⟨IH⁻⟩. Similar results are obtained for the binding of the acetamidate ion, for which a bidentate binding conformation is observed in the presence of Be^{2+} and Thr 199 (⟨IIC⁻⟩ and ⟨III⁻⟩, Figures 3 and 5), while a monodentate binding conformation is favored when three histidine ligands are included (⟨IIJ⁻⟩ and ⟨IIK⁻⟩, Figure 5). However, the active-site residues have negligible effects on the binding conformation of the acetamide molecule, for which a consistent binding conformation with the carbonyl oxygen coordinated to the fifth coordination site of the metal ion is obtained. In sum, local interactions between the inhibitor and active-site residues and among active-site residues themselves are important in determining the binding conformation of the inhibitor. In addition, the active-site residues may affect the binding conformations of neutral and negatively charged inhibitors differently.

In our previous calculations (Liang & Lipscomb, 1987), we have found that although inclusion of diffuse orbitals on the heavy atoms in the 4-31G basis set, yielding the 4-31G+ basis set, lowers the energies of anionic molecules, the stabilizing effects cancel in the evaluation of relative energies. In the study of proton transfer in $H_3O_2^-$ (Szczešniak & Scheiner, 1982), $H_5O_2^+$ (Scheiner, 1981), and NH_4H_2O (Scheiner, 1982), 4-31G calculations were shown to reproduce the barriers obtained from calculations including extended basis set and correlation energies. Although no general conclusion that the 4-31G basis is adequate can be drawn, we expect that the qualitative properties are preserved, in view of the large energy differences (20–50 kcal/mol) between the most stable conformer and other conformers (Tables I and IV).

It is hoped that studies of inhibitor binding would improve the understanding of drug binding and substrate binding of CO_2 to carbonic anhydrase. CO_2 has long been thought to bind as its neutral competitive inhibitor, imidazole, to the fifth coordination site of the metal ion (Kannan et al., 1977). Eriksson et al. (1987), on the basis of their X-ray structure of the AMSulf–HCA II complex, have further suggested that the specific binding positions of the two oxygen atoms of CO_2 resemble those of the two oxygen atoms of sulfonamide. Studies by NMR of $^{13}CO_2$ binding to Cu^{2+}-substituted HCA (Bertini et al., 1987) and of HCO_3^- binding to CO^{2+}-substituted HCA I (Stein et al., 1977; Williams & Henkens, 1985) have also implied a metal–oxygen distance of 3–4 Å. In addition, Pullman's theoretical studies yielded a Zn^{2+}–O distance of 2.88 Å (Pullman, 1981) as compared with our 2.64 Å (Liang & Lipscomb, 1989) for the zinc-bound CO_2. A large Be^{2+}–O distance of 2.99 Å is also obtained here for Be^{2+}-bound acetamide. All of these results suggest that CO_2 binds weakly at a large Zn^{2+}–O distance to the fifth coordination site of the metal ion. To further understand the binding of CO_2, molecular dynamics simulations and structural studies of CO_2–HCA II complexes at high gas pressures may be informative.

The kinetic studies of the binding of six homologous series of sulfonamide compounds to carbonic anhydrase have led King and Burgen to a two-step binding mechanism (Taylor et al., 1970a; King & Burgen, 1976), which involves (1) the initial binding of sulfonamide as neutral species to the hydrophobic pocket of the active site and (2) the subsequent deprotonation of sulfonamide and coordination of the sulfonamidate ion to the metal ion. This two-step binding mechanism is supported by the observations (a) that sulfonamides can bind to the apoenzyme as well as to the holoenzyme [the X-ray structure of the apoenzyme is isomorphous with that of the holoenzyme (Kannan et al., 1971)], (b) that binding to the apoenzyme is pH independent, and (c) that changes in binding constants to the holoenzyme within the same ho-

mologous series are largely reflected by changes in binding constants to the apoenzyme (King & Burgen, 1976). It was found that step 2, which is both pH dependent and rate limiting (Taylor et al., 1970b; Kernohan, 1966; Lindskog & Thorslund, 1968), has an estimated barrier of ~9 kcal/mol (King & Burgen, 1976). The detailed mechanism of step 2 remains unclear as to whether deprotonation of sulfonamide and metal coordination of the sulfonamidate ion take place sequentially or concertedly.

In the remainder of this discussion we consider the three-step binding mechanism of amide compounds, which has been described in the introduction (Figure 6). Rogers et al., on the basis of their spectroscopic studies of the binding of iodoacetamide and ethyl carbamate, suggested that deprotonation of the amide compounds occurs before their final coordination to the metal ion. This binding gives rise to large spectral changes in the metal ion (Rogers et al., 1987). However, the pK_a value of the amide group is ~14–15, for which a maximum rate of 10^{-6} s^{-1} is expected for spontaneous deprotonation, assuming a diffusion-limited protonation rate of 10^9 M^{-1} s^{-1}. Thus, most of the amide compounds would remain protonated in the initial binding to the active-site metal ion. Our theoretical studies have indicated that acetamide can bind as the neutral species in which the carbonyl oxygen binds to the fifth coordination site of the metal ion: in complex ⟨IIH⟩ (Table IV and Figure 5) the values of Be^{2+}–O = 2.99 Å and a bond order of Be^{2+}–O = 0.007 indicate a weak Be^{2+}–O interaction. This weak interaction between the metal ion and the amide compound in the initial binding probably would not induce large spectral changes of the metal ion, and thus the experimentally observed spectral changes may arise primarily from final coordination of the deprotonated amidate compound through amide nitrogen to the metal ion (Be^{2+}–N = 1.57 Å in ⟨IIK$^-$⟩, Figure 5). It was also shown in Sigel and Martin's studies (1982) of metal ion complexes with peptides and amide compounds that neutral amide compounds bind weakly through carbonyl oxygens to the metal ion, while the deprotonated amidate compounds bind tightly through amide nitrogens to the metal ion. We thus propose for step 1 of the binding mechanism a weak binding of the neutral amide compound through the carbonyl oxygen to the fifth coordination site of the metal ion.

Immediately following metal coordination, the pK_a value of the coordinated amide compound is expected to be lowered. In our calculations, the proton affinity of 392 kcal/mol for a neutral unbound acetamide molecule is reduced to 151 kcal/mol when the carbonyl oxygen is coordinated to Be^{2+}. In Sigel and Martin's studies (1982), the pK_a values of 14–15 for unbound amide compounds are lowered to 10–11 when the carbonyl oxygen is coordinated to the metal ion. In addition, the pK_a value of 14 for the free mononegative oxamate ion is lowered to 9.5 in the binding of oxamate to the metal ion of carbonic anhydrase (Wolpert et al., 1977; Rogers et al., 1987). These results suggest a plausible metal-facilitated amide deprotonation reaction, which is proposed in our three-step binding mechanism to proceed through proton transfer from the amide nitrogen to the metal-bound OH^- (step 2, Figure 6). The barrier of this proton-transfer process (Table VI), estimated at the 4-31G SCF MO level, may account for the experimentally observed slow association kinetics of amide compounds.

Rogers et al. have ruled out the possibility that conformational changes of HCA I are rate limiting in the binding of amide compounds (Rogers et al., 1987). Steric hindrance during the release of metal-bound H_2O is also unlikely to be rate limiting, because sulfonamide, which is larger than iodoacetamide and is, therefore, expected to induce more steric hindrance, is known to have a larger association rate constant than iodoacetamide. As mentioned above, the rate-limiting step of sulfonamide binding consists of deprotonation of sulfonamide and coordination of the sulfonamidate ion to the active-site metal ion. The observed different association rate constants between amide and sulfonamide compounds may reflect the different pK_a values of these inhibitor compounds.[4] It is important to point out that our three-step binding mechanism of the amide compound, although successful in explaining most of the experimental results, requires further investigation to consolidate its validity and importance. Future studies on kinetic deuterium isotope effects in the binding of deuterated inhibitors and on pK_a changes of the amide compounds upon metal coordination, as well as theoretical modeling and simulations of binding conformations and binding processes of amide compounds to the active site of carbonic anhydrase, as essential to better understand the detailed picture of inhibitor–enzyme interactions.

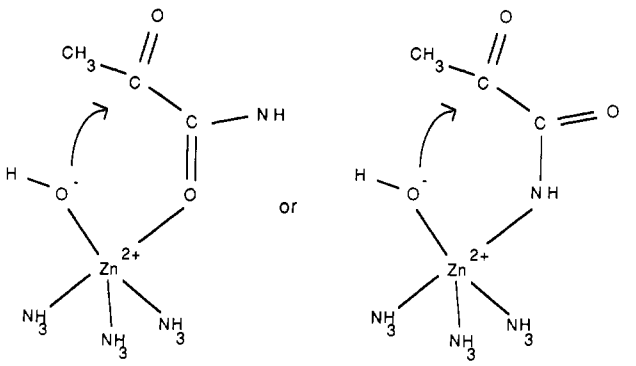

FIGURE 8: Possible binding conformation of the pyruvamidate ion on the metal ion in the active site of carbonic anhydrase. HCA I is known to catalyze the hydration reaction of pyruvamide to form the *gem* diol.

It is known that in aqueous solution coordination of metal ions to the carbonyl oxygen facilitates the hydrolysis of amide compounds, while coordination of metal ions to the amide nitrogen inhibits such hydrolysis. In the binding of amide compounds to the active-site metal ion of carbonic anhydrase, no hydrolysis was detected. This absence of hydrolytic activity toward amide compounds may imply a special binding conformation of the amide compound, in which the distance between the metal-bound OH^- and the amide hydrogen (~1.6–1.9 Å in acetamide binding) is much shorter than that between the metal-bound OH^- and the carbonyl carbon (>2.5 Å in acetamide binding); as a result, proton transfer from the amide nitrogen to the metal-bound OH^- is favored over nucleophilic attack from the metal-bound OH^- to the carbonyl carbon that leads to amide hydrolysis. Similar considerations may explain the absence of proteolytic activities of carbonic anhydrase toward peptides. Finally, Mukherjee et al. (1987) have shown that HCA I catalyzes the hydration of pyruvamide (K_i = 0.1 mM) to form the *gem* diol. It is expected that binding of pyruvamide as anionic species to the metal ion through the carbonyl oxygen or amide nitrogen (Figure 8) would place the β carbon adjacent to the metal-bound OH^- for a direct nucleophlic attack.

[4] For example, the sulfonamide compounds with pK_a of ~9–11 have association rate constants of 10^6–10^9 M^{-1} s^{-1}, while the amide compounds with pK_a of 14–15 have association rate constants of 1–10 M^{-1} s^{-1}. Of course, binding of the hydrophobic group of the sulfonamide compound to the hydrophobic pocket in carbonic anhydrase may also contribute to its fast and tight binding.

ACKNOWLEDGMENTS

We thank Dr. E. A. Eriksson and Professors T. A. Jones and A. Liljas for providing the 2.0-Å resolution coordinates of AMSulf–HCA II complex and Professor Raja G. Khalifah for his useful discussion.

Registry No. HCA II, 9001-03-0; Zn, 7440-66-6; sulfonamide, 637-74-1; acetamide, 60-35-5.

REFERENCES

Bertini, I., & Luchinat, C. (1983) *Acc. Chem. Res. 16*, 272.
Bertini, I., Luchinat, C., Roelens, S., & Moratal, J. M. (1987) *J. Am. Chem. Soc. 109*, 7855.
Blackburn, B., Mann, B. E., Taylor, B. F., & Worrall, A. F. (1985) *Eur. J. Biochem. 153*, 553.
Coleman, J. E., et al. (1980) in *Biophysics and Physiology of Carbon Dioxide* (Bauer, C., Gros, G., & Bartels, H., Eds.) pp 133–285, Springer, Berlin.
Cruickshank, D. W. J. (1961) *J. Chem. Soc.*, 5486.
Ditchfield, R., Hehre, W. J., & Pople, J. A. (1971) *J. Chem. Phys. 54*, 724.
Edelhoch, J. L., Bocian, D. F., & Sudmeier, J. L. (1981) *Biochemistry 20*, 4951.
Eriksson, E. A. (1988) Structural Differences between High and Low Activity Forms of Carbonic Anhydrase, Ph.D. Thesis, Uppsala University, Uppsala, Sweden.
Eriksson, E. A., Jones, T. A., & Liljas, A. (1986) in *Zinc Enzymes* (Bertini, I., Luchinat, C., Maret, W., & Zeppezauer, M., Eds.) pp 317–328, Birkhauser, Boston.
Eriksson, E. A., Jones, T. A., & Liljas, A. (1989) *Protein 4*, 274.
Forsman, C., Behravan, G., Jonsson, B.-H., Liang, Z.-W., Lindskog, S., Ren, X., Sandström, V., & Wallgren, K. (1988) *FEBS Lett. 229*, 360.
Harrington, P. C., & Wilkins, R. G. (1980) *J. Inorg. Biochem. 12*, 107.
Hehre, W. J., Stewart, R. F., & Pople, J. A. (1969) *J. Chem. Phys. 51*, 2657.
Kanamori, K., & Roberts, J. D. (1983) *Biochemistry 22*, 2658.
Kannan, K. K. (1979) in *Biophysics and Physiology of Carbon Dioxide* (Bauer, C., Gros, G., & Bartels, H., Eds.) pp 184–205, Springer, Berlin.
Kannan, K. K., Liljas, A., Waara, I., Bergstēn, P. C., Lövgren, S., Strandberg, B., Bengtsson, U., Carlbom, U., Fridborg, K., Järup, L., & Petef, K. (1971) *Cold Spring Harbor Symp. Quant. Biol. 36*, 221–231.
Kannan, K. K., Waara, I., Notstrand, B., Lövgren, S., Borell, A., Fridborg, K., & Petef, M. (1977) in *Drug Action at the Molecular Level* (Roberts, G. C. K., Ed.) pp 73–91, McMillan, London.
Kannan, K. K., Petef, M., Fridborg, K., Cid-Dresdner, H., & Lövgren, S. (1977) *FEBS Lett. 73*, 115.
Kernohan, J. C. (1966) *Biochim. Biophys. Acta 118*, 405.
King, R. W., & Burgen, A. S. V. (1976) *Proc. R. Soc. London B193*, 107.
Liang, J.-Y., & Lipscomb, W. N. (1987) *Biochemistry 26*, 5293.
Liang, J.-Y., & Lipscomb, W. N. (1989) *Int. J. Quant. Chem.* (in press).
Lindskog, S. (1983) in *Zinc Enzymes* (Spiro, T. G., Ed.) p 77, Wiley New York.
Lindskog, S., & Thorslund, A. (1968) *Eur. J. Biochem. 3*, 453.
Lindskog, S., Engberg, P., Forsman, C., Ibrahim, S. A., Jonsson, B.-H., Simonsson, I., & Tibell, L. (1984) *Ann. N.Y. Acad. Sci. 429*, 61.
Lipscomb, W. N. (1983) *Annu. Rev. Biochem. 52*, 17.
Mukherjee, J., Rogers, J. I., & Khalifah, R. G. (1987) *J. Am. Chem. Soc. 109*, 7232.
Mulliken, R. S. (1955) *J. Chem. Phys. 23*, 1833.
Pocker, Y., & Stone, J. T. (1968) *Biochemistry 7*, 2936.
Pocker, Y., & Sarkanen, S. (1978) *Adv. Enzymol. Relat. Areas Mol. Biol. 47*, 149.
Prince, R. H. (1979) *Adv. Inorg. Chem. Radiochem. 22*, 349.
Pullman, A. (1981) *Ann. N.Y. Acad. Sci. 367*, 340.
Pullman, A., & Demoulin, D. (1979) *Int. J. Quant. Chem. 16*, 641.
Rogers, J. I., Mukherjee, J., & Khalifah, R. G. (1987) *Biochemistry 26*, 5672.
Sanyal, G., Swenson, E. R., Pessah, N. I., & Maren, T. H. (1982) *Mol. Pharmacol. 22*, 211.
Scheiner, S. (1981) *J. Am. Chem. Soc. 103*, 315.
Scheiner, S. (1982) *J. Phys. Chem. 86*, 376.
Sigel, H., & Martin, R. B. (1982) *Chem. Rev. 82*, 385.
Silverman, D. N., & Lindskog, S. (1988) *Acc. Chem. Res. 21*, 30.
Stein, P. J., Merrill, S. P., & Henkens, R. W. (1977) *J. Am. Chem. Soc. 99*, 3194.
Szcześniak, M. M., & Scheiner, S. (1982) *J. Chem. Phys. 77*, 4586.
Taylor, P. W., & Burgen, A. S. V. (1971) *Biochemistry 10*, 3859.
Taylor, P. W., King, R. W., & Burgen, A. S. V. (1970a) *Biochemistry 9*, 2638.
Taylor, P. W., King, R. W., & Burgen, A. S. V. (1970b) *Biochemistry 9*, 3894.
Taylor, P. W., Feeney, J., & Burgen, A. S. V. (1971) *Biochemistry 10*, 3866.
Vedani, A., & Dunitz, D. (1985) *J. Am. Chem. Soc. 107*, 7653.
Verpoorte, J. A., Mehta, S., & Edsall, J. T. (1967) *J. Biol. Chem. 242*, 4221.
Whitney, P. L. (1970) *Eur. J. Biochem. 16*, 126.
Whitney, P. L. (1973) *J. Biol. Chem. 248*, 2785.
Whitney, P. L., Folsch, G., Nyman, P. O., & Malmstrom, B. G. (1967) *J. Biol. Chem. 242*, 4206.
Williams, T. J., & Henkens, R. W. (1985) *Biochemistry 24*, 2459.
Wolpert, H. R., Strader, C. D., & Khalifah, R. G. (1977) *Biochemistry 16*, 5717.